

# Metrics on End-Periodic Manifolds as Models for Dark Matter

Christopher L. Duston 

Department of Physics, Merrimack College, North Andover, MA 01845, USA; dustonc@merrimack.edu

**Abstract:** In this paper we will detail an approach to generate metrics and matter models on end-periodic manifolds, which are used extensively in the study of the exotic smooth structures of  $\mathbb{R}^4$ . After an overview of the technique, we will present two specific examples, discuss the associated matter models by solving the Einstein equations, and determine the physical viability by examining the energy conditions. We compare the resulting model directly with existing models of matter distributions in extragalactic systems, to highlight the viability of utilizing exotic smooth structures to understand the existence and distribution of dark matter.

**Keywords:** general relativity; differential geometry; exotic smooth structure; dark matter; gravitational lensing

## 1. Introduction

The understanding of our physical Universe as fundamentally a question of geometry is rooted in the key quantitative tool we have to study it, General Relativity (GR). Not only are space and time inexorably linked into a single geometric structure, which dictates how matter moves through it, but the matter content influences that geometric structure directly. Through the development of GR, as physicists have been amassing evidence for it's physical validity, mathematicians have been studying it's formal structure. These formal structures start with the 4D spacetime manifold, and have now branched out into the study of fiber bundles, spinors, strings, and noncommutative algebras, among many others. All of these areas have very well-developed physical motivations as well as mathematical explorations and rigor.

A particular example of an interesting and productive avenue of mathematical exploration has been that of exotic smooth structures. In brief, an exotic smooth structure of a manifold  $M$  is a smooth manifold  $M_\theta$  for which a map between them  $f : M \rightarrow M_\theta$  can only be found to be continuous, not smooth (for a more extensive introduction to this topic, see [1,2]). This relationship between  $M$  and  $M_\theta$  means they share the same topology (large-scale structure), but are inequivalent under diffeomorphisms (small-scale structure), the gauge symmetry of GR. In addition, by evidently evading the various uniqueness theorems associated with the existence of a Cauchy surface [3], these spacetimes are necessarily non-globally hyperbolic. Metrics on  $M_\theta$  would be inequivalent solutions to the Einstein equations, despite the two spacetimes having the same topological structure. Specifically, physical predictions requiring the use of derivatives (which characterizes most predictions in physics) would not match on the two manifolds.

Although a seemingly esoteric phenomena, exotic smooth structure has been extensively studied and marveled at in the mathematical community for many years. The first examples were discovered in dimension 7 in 1956 by John Milnor [4], with work in dimension 4 occurring the 1980s and 1990s [5–7]. At this point, there had been little discussion regarding how these structures might impact physical models of our Universe. One of the major complications was the manner of presentation of the available examples—they were very abstract, lacking sufficient details regarding the local geometry that would be needed to define a metric. Early progress was made by Schleich and Witt [8], who used the 7-dimensional Wallach spaces  $SU(3)/i_{k,l}(\mathbb{S}^1)$  with an embedding  $i_{k,l} : \mathbb{S}^1 \rightarrow SU(3)$



**Citation:** Duston, C.L. Metrics on End-Periodic Manifolds as Models for Dark Matter. *Universe* **2022**, *8*, 167. <https://doi.org/10.3390/universe8030167>

Academic Editors: Torsten Asselmeyer-Maluga, Jerzy Król and Douglas Singleton

Received: 23 December 2021

Accepted: 4 March 2022

Published: 8 March 2022

**Publisher's Note:** MDPI stays neutral with regard to jurisdictional claims in published maps and institutional affiliations.



**Copyright:** © 2022 by the author. Licensee MDPI, Basel, Switzerland. This article is an open access article distributed under the terms and conditions of the Creative Commons Attribution (CC BY) license (<https://creativecommons.org/licenses/by/4.0/>).

that winds  $\mathbb{S}^1$  around a maximal torus in  $SU(3)$  according to the integers  $k, l$ . Through an analysis of the characteristic classes of these spaces it was known that some sets of these spaces were exotic (that is, homeomorphic but not diffeomorphic), and also that they admitted Einstein metrics. As coset spaces, it was possible to find a metric explicitly, and they constructed a semi-classical model in Euclidean quantum gravity to demonstrate that the inclusion of the exotic structures impacted a physical observable (specifically, the expectation value of volume).

Progress in 4-dimensions took somewhat longer. A key approach was initiated by Salvetti [9], who used iterated branched covers of  $\mathbb{C}\mathbb{P}^2$  to calculate the Seiberg-Witten invariants [7] and prove there were an infinite number of exotic smooth structures presented in this way. This branched cover  $\pi : M \rightarrow N$  construction over a manifold  $N$  with metric  $g$  easily leads to a metric  $\pi^*g$  over a particular cover  $M$ , and this technique was then used to create a model inspired by Schleich and Witt, but this time in four-dimensions [10]. The findings were similar—the inclusion of exotic smoothness structures impacted a physical observable, at least semi-classically.

It's worth mentioning a parallel track of research to access the physical implications of exotic smooth structure, in which knowledge of the metric is foregone in favor of knowledge of the action [11–14]. Briefly, this approach uses techniques from knot theory and surgery to construct exotic smooth structures, and then considers what happens to the curvature under the various actions on the embedded or immersed submanifolds. Using these techniques, a wide variety of interesting phenomena can be developed—for example, exotic smooth structures can be seen to mimic the inclusion of fermions in spacetime, or predict values for the cosmological constant. This is a formally different approach than we will be taking in the present work, and has been included here primarily for context.

So while this brief overview should make it clear that progress is being made, we have not presented any solid predictions of a particular observation which might be explained by exotic smooth structure. The most important possibility for this is undoubtedly that of Brans [15], which has come to be known as The Brans Conjecture. It is based on the idea that so-called “small exotic  $\mathbb{R}^4$ ” can be embedded in regular  $\mathbb{R}^4$ , and photons crossing the boundary would be deflected as they crossed. One consequence of this conjecture is that this effect would be observed as gravitational lensing, with the source of the lensing not being matter, but rather this exotic manifold structure. Since excess gravitational lensing is attributed to the existence of dark matter [16], the Brans Conjecture represents an alternative explanation for this excess lensing that does not require new or exotic particles or interactions. Since direct experimental searches for these exotic particles have consistently failed to find evidence for them (at the LHC, for example [17]), exploring manifestations of the Brans conjecture is looking more attractive.

It should also be clarified what the Brans conjecture represents in the overall study of dark matter. Evidence for dark matter is found at essentially two different astrophysical scales—the galactic and the cosmological. At the galactic scale, this comes in the form of rotation curves of spiral galaxies [18], or gravitational lensing [19,20]. At the cosmological scale, it comes (for example) in the form of the acoustic peaks in the Cosmic Microwave Background (CMB) [21]. The Brans conjecture is generally regarded to apply to just the first type of evidence, on galactic scales, rather than on cosmological scales. Of course, there is no reason that exotic smooth structure could not play a role in the study of the early universe ([22,23], for example), but the signal would presumably be cleaner at the galactic scale because the only physics involved there is that of the gravitational field, and only at relatively low energies. This is in contrast to the complex modeling required to understand the early universe and structure formation. So in this work we are not attempting to address every particular observational evidence we have for dark matter, only the evidence that appears at the galactic scale. This limitation is also true for many of the other approaches we will be discussing [2,13,24,25].

As an aside (and by way of comparison to the current study), there are several other viable alternatives to the existence of dark matter as “exotic matter” from the particle physics

perspective. We highlight two of these, the first being Modified Newtonian Dynamics (MOND) [26]. In MOND, the gravitational force is modified in low-density regions like the outer regions of a galaxy to match observations of galactic rotation curves (a relativistic version exists as well [27]). Another approach is  $f(R)$  gravity, which is actually a constellation of theories in which scalar functions of the curvature and/or connection are added to the Einstein-Hilbert action [28]. Both of these approaches have been successful in describing various aspects of dark energy and dark matter, but we want to emphasize that they are modifying the theory of gravity at the level of the action. This is in contrast to exotic smooth structures, which are alternative solutions to the standard Einstein-Hilbert action (although, as outlined below, sometimes these alternative solutions can be explicitly parameterized at the level of the action). One might classify MOND and  $f(R)$  theories as “exotic physics”, whereas exotic smooth structures might be classified as “exotic mathematics”.

In this paper we will be presenting a spacetime model (with a concrete metric and matter content) for such an exotic  $\mathbb{R}^4$ . It is based on earlier work [24], which clarified a technique for finding explicit metrics on end-periodic manifolds [29]. In the present work, we will be focusing on finding a valid matter model and comparing the model to those commonly used when studying dark matter, and we will see that the models are comparable at this initial level of analysis. Specifically, for one particular choice of building block we will find matter distribution matching a singular isothermal sphere.

In fact, the appearance of this particular matter distribution is not new in the field of exotic smooth structure; a recent study found the same using an entirely different approach [25]. In brief, that work starts with gravitational solitons in the weak-field limit, and uses a particular foliation to both construct the spacetime and demonstrate that the smoothness structure of the spacetime can be tracked by the Seiberg-Witten equations. Following this, the explicit presentation of the metric demonstrates that the matter distribution is again a singular isothermal sphere. We will point out the various and interesting similarities and differences in this approach compared with the one we are taking.

Beyond this introduction, this paper is organized as follows: Section 2 will briefly present the theoretical and mathematical background needed to understand the metric generation procedure on end periodic manifolds, and Section 3 will give some context for how this approach fits into the larger question, “what is the dynamical source of exotic smoothness structures?” We will then present two specific examples of this approach, using a Kruskal black hole (Section 4) and an embedded conformal surface (Section 5) as building blocks. A consistent matter model for the latter can be found in Section 6, and we will conclude by briefly summarizing our findings in Section 7.

## 2. Metrics on End-Periodic Manifolds

In this section we present the basic background and tools we are using to generate metrics on end-periodic manifolds, the Z-transformation<sup>1</sup>. This was first presented in [29], where it was used to prove that the number of exotic smoothness structures on  $\mathbb{R}^4$  is uncountably infinite. The approach was finally clarified for the physics community in [24,30], and we take this last reference as our primary starting point.

An end-periodic manifold is constructed with a building block 4-manifold  $W$  and a map  $i$  that identifies the ends of the building block,  $Y = W/i$ . The end-periodic manifold is the cover

$$\tilde{Y} = \dots \cup_N W_{-1} \cup_N W_0 \cup_N W_1 \cup_N \dots$$

with projection  $\pi : \tilde{Y} \rightarrow Y$ . We also have a map  $T : W_i \rightarrow W_{i+1}$  which identifies the copies of the building block (this map is also used to define the end-periodic bundles in the original work of [29], and the specific details about the map  $T$  can be found there or in [24]). We will pick the metric on the building block  $W$  to be  $\hat{g}$ , which we first have to extend to  $Y \times \mathbb{C}^*$  to keep track of the order of the cover. We will do this by making one

of the coordinates complex and denote this metric  $\hat{g}_z, z \in \mathbb{C}^* = \mathbb{S}^1$ . Since this metric is periodic, we can define a transformation

$$\hat{g}_z = \sum_{n=-\infty}^{n=\infty} z^n (T^n g),$$

where  $g$  is the metric on  $Y$  and  $T^n g$  is the metric on the block  $n$ . We can invert this expression in a formal way to determine the metric on each block,

$$T^n g = \frac{1}{2\pi i} \oint_{|z|=s} z^{-n} \hat{g}_z \frac{dz}{z}. \tag{1}$$

This expression is independent of the magnitude of the complex coordinate  $|z| = s$  thanks to Cauchy’s theorem (note that compared to the conventional Z-transformation we have here exchanged  $z \leftrightarrow 1/z$  in these two expressions to match what was done originally in [29]).

We would like to mention one aspect of this approach (initially outlined by [24]) that differs from the original presentation by Taubes, and that is the use of a Lorentzian metric rather than Riemannian. Although the proof of the existence of the exotic smooth structures in [29] did use a metric with a positive signature, the obstruction to finding a Lorentzian metric is topological, and should be independent of the signature of the metric (specifically, we need a nowhere vanishing timelike vector field-further details can be found in [13]). Further, there is a simple argument that a Wick rotation of the metric will pass unaffected through the Z-transformation. Following the basic argumentation of [31], we can define the “not quite Lorentzian metric”

$$g_\epsilon = g_L + i\epsilon \frac{V \otimes V}{g_L(V, V)}$$

associated to the Lorentzian metric  $g_L$  and timelike vector field  $V$ . For example, in the cases discussed in this paper we could take  $V = (1/\sqrt{g_{00}}, 0, 0, 0)$ , and the Z-transformation on that component of the metric will be

$$\frac{1}{2\pi i} \oint_{|z|=s} \frac{1}{z^{n+1}} (- (1 + i\epsilon) g_{00}) dz = \frac{-(1 + i\epsilon)}{2\pi i} \oint_{|z|=s} \frac{1}{z^{n+1}} g_{00} dz.$$

It is then relatively easy to see that a transition from a Lorentzian metric ( $\epsilon = 0$ ) to a Riemannian ( $\epsilon = 2i$ ) just needs to satisfy the same conditions that as a usual Wick rotation-namely, that one avoids  $\epsilon = i$ .

The next step is to pick an appropriate building block  $W$  and metric  $\hat{g}$ , and decide which part of the metric is going to be periodic. In [24], the metric choice was Kruskal and the complex coordinate was chosen to be  $z = exp(ir)$  with the Kruskal coordinate  $v$  tracking the order of the cover. This choice lead to some singular structure in the form of a Heaviside function, suggesting a dimensional reduction from 4 to 2. This dimensional reduction is associated to the a collapse of the 3D hyperbolic spatial section into a 1D tree in the large curvature limit [30], and may have interesting implications for the quantum theory [32]. In Section 4 we will take an alternative approach and discuss the differences.

### 3. Perspective Taken in This Paper

The Einstein equation tells us the equality between the matter model of the Universe and the geometry (with the cosmological constant being interpreted either way). The traditional way to solve the Einstein equation is to impose symmetries (or Killing vectors) on this system of equations to simultaneously solve for both the matter and geometry together. However, doing this does not usually furnish a complete description of the matter content. For example, a traditional solution for the FLRW provides the scale factor as a function of the density and pressure of an ideal fluid, but does not yet tell us what the matter *content* of the model is. For the case of FLRW, we often have a mixture of radiation,

matter, and cosmological constant (as well as more exotic options, see for example [33]). Typically observations are required to determine the actual matter content in a particular relativistic model.

Due to the tool we have available to us in the study of end-periodic manifolds, we are going to be taking a slightly different perspective on solving the Einstein equations. The Z-transformation generates new metrics on end-periodic manifolds, but it does not explicitly affect the matter model. Naturally, changing the metric must impact the matter content since that the system still solves the Einstein equation, but the point is that rather than starting with symmetries of spacetime, we are starting with a (hopefully new) metric, and then solving the Einstein equation. By doing this we will be finding a valid matter model (still likely without knowing the specific matter *content*) for a particular choice of geometry. The natural next steps would be to verify that the matter model is physically reasonable, and then checking to see if it can be used for our particular study-to model gravitational lensing without needing dark matter. Stated another way, a solution to the Einstein equations is simply the set of metric components  $g_{ab}$  and matter components  $T_{ab}$  that solves  $G_{ab} = 8\pi GT_{ab}$ , and we are going to be looking for a  $T_{ab}$  that corresponds to a particular  $g_{ab}$ , before actually asking what form  $T_{ab}$  should be for a given class of matter models.

A challenging aspect of this field is understanding what the “dynamical” source of this exotic smoothness actually is. As discussed in Section 1, they arise because of the existence of a continuous map

$$f : M \rightarrow N,$$

but the lack of a smooth one (diffeomorphism). As such, a metric  $g$  on  $N$  that solves the Einstein equations cannot be pulled back to a metric  $f^*g$  on  $M$  that is also a solution to the Einstein equations. In other words, solutions to the field equations on  $M$  are non-isometric to solutions on  $N$ . So how should we go about finding the exotic structures  $M$  associated to a particular manifold  $N$  with known geometric structures? If we knew what the continuous map  $f$  was (or say  $C^1$  so the pullback was defined), we could use  $f^*g$ , but not only are such maps typically not part of the construction of exotic smooth structures, that implies that  $f^*g$  would at least not be  $C^\infty$ , raising questions about how it could solve the field equations at all.

Some clarification might come from considering what happens at the level of the action. For a pair of exotic smooth structures  $M_1$  and  $M_2$ , being non-diffeomorphic means the equation

$$\delta S(g) = \delta(S(g)_{EH} + S(g)_M) = 0$$

for the Einstein-Hilbert action  $S_{EH}$  and matter action  $S_M$ , must have different solutions  $g_1, g_2$ . However, what kinds of differences in the action would lead to alternative solutions? First, let us restrict our considerations to cases in which the matter content does not change—that is,  $S(g_1)_M = S(g_2)_M$ . This is consistent with our perspective in this paper, since one could consider the matter action to be independently verified by observations (in the specific case of gravitational lensing, by mass-to-light ratios). If we are therefore just considering what happens to the Einstein-Hilbert action  $S_{EH}$ , based on the discussion in the introduction it appears we have two essential cases:

1. Explicit differences in the action that are parameterized by the construction of the exotic structure. In other words,

$$S(g_1)_{EH} - S(g_2)_{EH} = F(\text{geometric parameters}).$$

For a specific example of this, we briefly discuss [14], in which there is an additional term in the action that takes the form

$$\int_{U(\Sigma)} \Phi D^{U(\Sigma)} \Phi dV.$$

Here  $\Sigma$  is an embedded 3-manifold in a neighborhood  $U(\Sigma) \subset M$ , which is described via a Weierstrass representation with the spinor  $\Phi$ . What is important about this characterization is that the geometric parameters of the construction of the exotic smooth structure appear as an extra term in the action. Thus, **the dynamical source of the exotic structure is the geometric construction of the structure-surgery, knots, framing, handles, etc.** Incidentally, in the work of [25], the dynamical source is the non-orthogonal vector fields on the leaves of a foliation.

2. Differences in the action which cannot be explicitly parameterized as above. In short, these are inequivalent solutions to the Einstein equations which do not have any apparent simple parameterization at the level of the action—one would expect them to have different curvature invariants, for example. Since the field equations are only sensitive to local geometry, the fact that they are topologically identical must come from their abstract presentation. Therefore in this case **the dynamical source of the exotic structure are local minima in the solution space of the Einstein-Hilbert action**, for a fixed topological background. The primary examples for this second category are found in the semi-classical models, such as [8,10,34].

We are not suggesting these are the only two possibilities, but they contain all known examples (either the action can be presented differently or not) and provide a useful framework to think about the source of exotic smooth structure. In this paper, we are focusing on the second case, and in the future work we will perform a similar analysis for the first case, to bring models in both categories closer to potential observational verification.

#### 4. The Exotic Kruskal Metric

We will first use the Z-transformation, presented in Section 2, with the Schwarzschild metric in Kruskal-Szekeres coordinates as our building block:

$$ds^2 = \left(\frac{32G^3M^3}{r}\right) \exp\left(-\frac{r}{2GM}\right) (-dT^2 + dR^2) + r^2 d\Omega^2,$$

where the radius is implicitly defined via

$$T^2 - R^2 = \left(1 - \frac{r}{2GM}\right) \exp\left(\frac{r}{2GM}\right).$$

We choose the  $(T, R)$  part of the metric to be periodic, tracked by the integer part of the timelike coordinate  $n = \lfloor T \rfloor$  (the lower brackets here indicate the floor function). For the complex coordinates, we will simply complexify the radius by setting  $r = zr_0$  for  $r_0 = 2GM$ , so that  $|r/r_0| = s$  is unitless. This should be compared with the original choice in [24], which was  $z = \exp(ir)$ . That choice leads to a natural logarithm in the denominator and an essential singularity in the inverse transformation.

With our choice  $r = zr_0$ , our inverse transformation (1) becomes

$$\frac{16G^2M^2}{2\pi i} \oint \frac{\exp(-z)}{z^{2+n}} dz,$$

and we need to perform a pole analysis on this to determine the value of the integral. Immediately we see that there are no poles for  $n < -1$ , but for  $n \geq -1$  we can determine the pole structure by expanding the exponential:

$$\frac{\exp(-z)}{z^{2+n}} = \sum_{m=0}^{\infty} \frac{(-z)^m}{m!} \frac{1}{z^{2+n}} = \sum_{m=0}^{\infty} \frac{(-1)^m}{m!} z^{m-n-2}.$$

So for a given value of  $n$  we will have a simple pole in the term with  $m = 1 + n$ , with residue given by

$$\oint \frac{\exp(-z)}{z^{2+n}} dz = 2\pi i \frac{(-1)^{(1+n)}}{(1+n)!}, \quad n \geq -1.$$

As in [24] (and discussed at the end of Section 2), in these coordinates we have a dimensional reduction  $4 \rightarrow 2$  for certain values of the timelike coordinate  $T < -1$ . We can relate this region back to the original spacetime to create a spacetime diagram for this Exotic Kruskal metric, which is shown in Figure 1. Since the transformation blocks everything  $T < -1$ , the white hole that existed in the past of the usual Schwarzschild geometry does not exist.

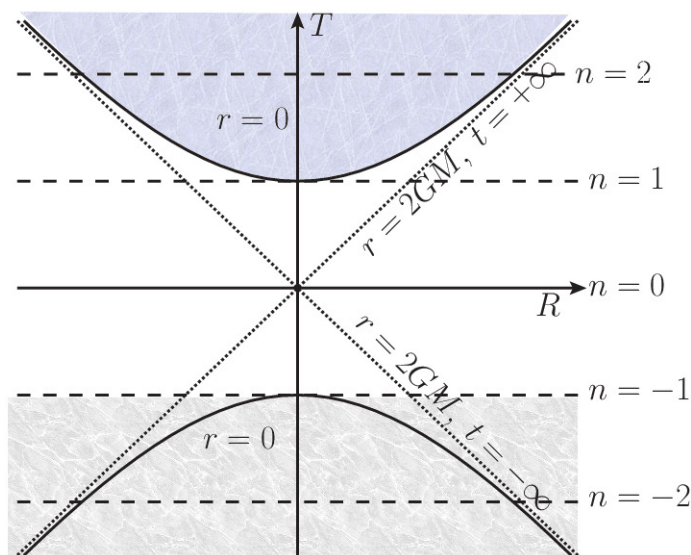


**Figure 1.** The Exotic Kruskal spacetime diagram with complex radial coordinate. The darkened region  $T < -1$  is absent due to a dimensional reduction in these two coordinates—the spacetime is simply a 2-sphere there.

The full exotic Kruskal metric is therefore

$$ds^2 = \begin{cases} \frac{(-1)^{(1+n)}}{(1+n)!} (16G^2M^2)(-dT^2 + dR^2) + r^2d\Omega^2 & T \geq -1 \\ r^2d\Omega^2 & T < -1 \end{cases} \quad (2)$$

Note that this metric is not yet a solution to the Einstein equations, since we have not yet specified an appropriate stress-energy tensor. The form of this metric is slightly different from [24], due to the differences discussed above in the choice of periodic variables. In principle, the next step here would be to find a matter model amenable to this metric, starting with options like pressureless dust and perfect fluids, moving on to anisotropic options. However, because  $r$  is defined implicitly in terms of  $(T, R)$ , this metric is quite complicated and is likely to fail. More explicitly, if we move back to the physical  $(t, r)$  coordinates, the metric becomes relatively complicated:

$$g = \frac{re^{\left(\frac{r}{2Gm}\right)}}{2Gm(n+1)!} \left\{ -\left(1 - \frac{2Gm}{r}\right) dt^2 + \left(1 - \frac{2Gm}{r}\right)^{-1} dr^2 \right\} + r^2d\Omega^2 \quad (3)$$

We will not attempt to solve the field equations for this metric here, but draw some inspiration from (2): our formulation of the Z-transformation produces a conformal transformation on the  $\mathbb{R}^2$  part of the spacetime. These types of metrics may have interesting properties in their own right (for example, how might they play a role in conformal gravity [35]?), but we will instead use this as inspiration for another choice of our building block metric in the next section.

### 5. A Building Block with a Locally Embedded Conformal Surface

Based on the appearance of a locally embedded conformal surface after the Z-transformation in the exotic Kruskal Metric (2), we will consider building blocks of

our end periodic manifold  $\mathcal{M}$  that produce these same structures more generally. We consider situations when the end period manifold has a metric that looks like

$$ds^2 = Z(t, r)(-dt^2 + dr^2) + r^2 d\Omega^2,$$

where  $Z(t, r)$  is the result of some Z-transformation on the  $n$ th block,

$$Z(t, r) = T^n g = \frac{1}{2\pi i} \oint_{|z|=s} z^{-n} \hat{g}_z \frac{dz}{z}.$$

Mimicking what we have done so far with Kruskal, let us start with a building block with topology  $\mathbb{R}^2 \times \mathbb{S}^2$ ,

$$ds^2 = g(t, r)(-dt^2 + dr^2) + r^2 d\Omega^2.$$

Further, let us continue to suppose the order of the transformation is tracked by the time coordinate ( $n = \lfloor t \rfloor$ ), we will complexify by  $r \rightarrow z \in \mathbb{C}$ , and additionally that our metric function is separable,  $g(t, r) = f(t)g(r)$ . We also suppose that  $g(r)$  is analytic in a region  $r_1 < |r - r_0| < r_2$  around a singular point  $r_0 = |z_0|$ , so its complexification will have a Laurent series

$$g(z) = \sum_{j=-\infty}^{j=\infty} g_j(z - z_0)^j, \quad g_j = \frac{1}{2\pi i} \oint_{\mathcal{C}} \frac{g(z') dz'}{(z' - z_0)^{j+1}}.$$

The transformation will then be

$$Z(t, r) = \frac{f(t)}{2\pi i} \oint_{|z|=r} g(z) z^{-(n+1)} dz = f(t)g_n, \quad n = \lfloor t \rfloor.$$

In other words, the effect of the transformation is to grab the  $n$ th term in the Taylor expansion of the metric on the building block, which will be specified by the time coordinate.

Under this transformation our metric is then

$$ds^2 = f(t)g_n(-dt^2 + dr^2) + r^2 d\Omega^2. \tag{4}$$

This will be the starting point for the later analysis. If  $f(t)$  is sufficiently well-behaved, we can shift the time and radial coordinates;

$$\begin{aligned} \bar{t} &= \int_{\lfloor t' \rfloor}^{\bar{t}} \sqrt{g_n f(t')} dt', & \bar{t} &= 0 \text{ at } t' = \lfloor t' \rfloor, & \bar{t} &< 1, \\ \bar{r} &= \sqrt{f(\bar{t})} g_n r, \\ ds^2 &= \left( \frac{\bar{r}^2 \dot{f}^2}{4f^2} - 1 \right) d\bar{t}^2 + d\bar{r}^2 - \frac{\bar{r} \dot{f}}{f} d\bar{r} d\bar{t} + \frac{\bar{r}^2}{f(\bar{t}) g_n} \Omega^2. \end{aligned} \tag{5}$$

Note that this transformation is  $\bar{t} = t - \lfloor t \rfloor$ , so that  $0 < \bar{t} < 1$  and the order of the cover  $n = \lfloor t \rfloor$  is constant. When  $\dot{f} = 0$ , this metric is equivalent to the Barriola-Vilenkin monopole [36],

$$ds^2 = -dt^2 + d\bar{r}^2 + (1 - \Delta) \bar{r}^2 (d\theta^2 + \sin^2 \theta d\phi^2),$$

which appears at this level to have an angle deficit that depends on time. When we look for a valid matter model in this case, we will see that the function  $f(t)$  must necessarily be constant. The scalar curvature for this geometry is

$$R = \frac{2 g_n f(t)^3 - r^2 \left( \frac{\partial f}{\partial t} \right)^2 + r^2 f(t) \frac{\partial^2 f}{\partial t^2} - 2 f(t)^2}{g_n r^2 f(t)^3}.$$

The curvature vanishes as  $r \rightarrow \infty$ , and is singular at  $r = 0$ . Additionally, for  $f(t) = 1/g_n$  the curvature is zero, but looking at (5) we see that this condition simply brings us back to Minkowski space.

Making a comparison to [25]; the metric (5) is similar to what is found in Section 5 of that paper, but with very different origins. In our case, we have performed a metric transformation and required that the resulting matter is reasonable, whereas the metric in [25] follows from the weak field limit of the optical metric. In either case, the result is essentially a metric with a conical angle deficit.

### 6. A Self-Consistent Matter Model for $\mathcal{M}$

As discussed in Section 3, the next step is to find a matter model for the metric (5) which satisfies the energy conditions. We don't want to yet enforce the static condition of  $f(t) = constant$ , but the metric is at least symmetric, so the Einstein tensor  $G_{\mu\nu}$  and the energy-momentum tensor will inherit that restrictions. Given that, one might start with a pressureless dust model with  $T_{00} = \rho(t, r)$  and  $T_{ij} = 0$ ; in this case the Einstein equations are (this and most of the following differential geometry calculations were done with SageMath [37]) ( $\kappa = 8\pi G$  here):

$$-g_n \kappa \rho f(t) + \frac{g_n f(t)}{r^2} - \frac{1}{r^2} = 0, \quad -\frac{g_n f(t)}{r^2} + \frac{1}{r^2} = 0, \quad \frac{r^2 \frac{\partial}{\partial t} f(t)^2}{2 g_n f(t)^3} - \frac{r^2 \frac{\partial^2}{(\partial t)^2} f(t)}{2 g_n f(t)^2} = 0.$$

To satisfy the second we require  $f(t) = 1/g_n$ , which not only implies a Minkowski metric, but also makes the density vanish in the first of these expressions. Trying an ideal fluid  $T_\nu^\mu = diag(\rho, P, P, P)$ , the same analysis leads to the field equations

$$-g_n \kappa \rho f(t) + \frac{g_n f(t)}{r^2} - \frac{1}{r^2} = 0, \quad -g_n \kappa P f(t) - \frac{g_n f(t)}{r^2} + \frac{1}{r^2} = 0, \\ -\kappa r^2 P + \frac{r^2 \frac{\partial}{\partial t} f(t)^2}{2 g_n f(t)^3} - \frac{r^2 \frac{\partial^2}{(\partial t)^2} f(t)}{2 g_n f(t)^2} = 0.$$

In this case the first equation implies  $\rho \propto \rho(t)/r^2$  and the second  $P \propto P(t)/r^2$ , but the energy conservation equation  $\nabla_\mu T_\nu^\mu = 0$  is

$$\left( -\frac{2 f(t) \frac{\partial \rho}{\partial t} + (T_0(t, r) + P(t, r)) \frac{\partial f}{\partial t}}{2 f(t)} \right) dt + \frac{\partial P}{\partial r} dr = 0,$$

telling us that  $\partial P / \partial r = 0$ , showing that the field equations are inconsistent.

At this stage, let us consider a matter model which is weakly anisotropic-specifically, the energy-momentum tensor in the radial direction is not identical to the angular directions:

$$T_\nu^\mu = \begin{pmatrix} -T_0(t, r) & & & \\ & T_1(t, r) & & \\ & & T_2(t, r) & \\ & & & T_2(t, r) \end{pmatrix} \tag{6}$$

Note that we should not automatically associate the component  $T_0$  with the matter density and  $T_i$  with fluid pressure- $T_1$  is the radial pressure, and  $T_2$  is the angular pressure, which accounts for possible anisotropies. This spacetime is Type I in the Hawking-Ellis classification [38], and see [39] for more on our approach to anisotropic stress-energy tensors. In fact, we could have expected this form of the energy-momentum tensor in the first place, since the spacetime we started with only had  $S^2$ -symmetry in the first place (not  $S^3$ ).

The energy conservation equation  $\nabla_\mu T_\nu^\mu = 0$  is

$$\left( -\frac{2f(t)\frac{\partial T_0}{\partial t} + (T_0(t,r) + T_1(t,r))\frac{\partial f}{\partial t}}{2f(t)} \right) dt + \left( \frac{r\frac{\partial T_1}{\partial r} + 2T_1(t,r) - 2T_2(t,r)}{r} \right) dr = 0, \tag{7}$$

and the Einstein equations are

$$\begin{aligned} -g_n \kappa T_0(t,r) f(t) + \frac{g_n f(t)}{r^2} - \frac{1}{r^2} &= 0 \\ -g_n \kappa T_1(t,r) f(t) - \frac{g_n f(t)}{r^2} + \frac{1}{r^2} &= 0 \\ -\kappa r^2 T_2(t,r) + \frac{r^2 \frac{\partial}{\partial t} f(t)^2}{2g_n f(t)^3} - \frac{r^2 \frac{\partial^2}{(\partial t)^2} f(t)}{2g_n f(t)^2} &= 0 \end{aligned}$$

It is immediately obvious that  $T_0 = -T_1$  (or  $\rho = P_r$ ), and further it appears  $T_0 \propto r^{-2}$  for the first field equation to be satisfied. So, setting

$$T_0(t,r) = \frac{K(t)}{r^2},$$

we can solve for the metric function

$$f(t) = \frac{1}{g_n(1 - \kappa K(t))}.$$

However, if we implement these two conditions in the energy conservation Equation (7), we find

$$-\frac{1}{r^2} \frac{\partial K(t)}{\partial t} dt - \frac{2T_2(t,r)}{r} dr = 0.$$

So  $T_2 = 0$  and  $K$  must be a constant, so the density is constant in time. Further,  $K \neq 1/\kappa$  or the conformal part of the metric will be singular.

Now we must demonstrate that this matter model satisfies some kind of energy condition. In our case we will choose the weak energy condition,

$$T_{\mu\nu} t^\mu t^\nu \geq 0,$$

for any timelike  $t^\mu$  as our criteria. Of course, this is the easiest one to satisfy, but without further physical constraints, passing this bar should be considered sufficient for the solution to be considered interesting. For us this expression reads

$$f g_n (T_0(t^0)^2 + T_1(t^1)^2) + r^2 T_2(t^2)^2 + r^2 \sin^2 \theta T_2(t^3)^2 \geq 0.$$

For a timelike vector, we have (this calculation is similar to that which one does for the energy conditions of the ideal fluid)  $f g_n (t^0)^2 = 1 + f g_n (t^1)^2 + r^2 (t^2)^2 + r^2 \sin^2 \theta (t^3)^2$ , so putting this into the expression above we arrive at

$$T_0 + f g_n (T_0 + T_1) (t^1)^2 + r^2 (T_0 + T_2) (t^2)^2 + r^2 \sin^2 \theta (T_0 + T_2) (t^3)^2 \geq 0.$$

So, this condition will surely be satisfied if  $T_0$  is positive, and if each of  $T_0 + T_i$  is also positive. If we choose  $K > 0$ , the radial pressure and density in this model are equal and positive,

$$\rho = P_r = \frac{K}{r^2} > 0.$$

So this model satisfies the weak energy condition (although minimally so).

The vanishing of the angular pressure  $T_2 = 0$  is a clear sign of the anisotropy, which we will briefly discuss. For a stress-energy tensor with anisotropic stress we have the generic equation [39]

$$T_{ab} = (\rho + p)u_a u_b + \pi_{ab},$$

where the anisotropy can be parameterized as

$$\pi_{ab} = \sqrt{3}S \left( c_a c_b - \frac{1}{3}(u_a u_b + g_{ab}) \right).$$

Here  $S$  is the magnitude of the anisotropy,

$$S = \sqrt{\frac{1}{2}|\pi_{ab}\pi^{ab}|}$$

and  $c_a = (0, \sqrt{g_{11}}, 0, 0)$  is a radial vector. In the comoving frame we have

$$T_0^0 = \rho, \quad T_1^1 = p + \frac{2}{\sqrt{3}}S, \quad T_2^2 = p - \frac{1}{\sqrt{3}}S,$$

where now  $p$  refers to the fluid pressure, rather than the radial pressure  $P_r$ . The vanishing of  $T_2$  simply indicates that the magnitude of the anisotropy is proportional to the fluid pressure,

$$S = \sqrt{3}p.$$

The source of the anisotropy could be self-interactions related to the microscopic details of the matter in question, and demonstrates the issue discussed in Section 3 about the lack of specific knowledge of the matter content. We do not want to go into extensive detail on that here, but we do want to mention one interesting option for the source of this anisotropy, and that is a perfect fluid combined with a massless scalar field with stress tensor

$$T_s^{\mu\nu} = \nabla^\mu \phi \nabla^\nu \phi - \frac{1}{2}g^{\mu\nu} \nabla_\rho \phi \nabla^\rho \phi.$$

Following [40], we can make the pressure vanish in the transverse direction by setting the fluid pressure to  $p_f = \frac{1}{2}(\nabla\phi)^2$ . This implies the radial pressure is equal to the energy density,  $p_r = \rho = (\nabla\phi)^2$ , as we found above. There is extensive literature on modeling dark matter as an ultra-light scalar field, which includes not just galaxy rotation curves and lensing, but also structure formation; for a brief review, see [41]. Finally, we want to point out that the presence of this anisotropy is a difference between our work and [25], which used a perfect fluid as the matter model, and found an equation of state with  $w = 0$ .

This matter distribution is an example of a polytropic equation of state,  $P \propto \rho^\gamma$ , with  $\gamma = 1$ , and is also known as the singular isothermal sphere. By solving the equation of hydrostatic equilibrium, it can be determined that our constant  $K$  is related to the central velocity distribution  $\sigma_v$  by [42]

$$K = \frac{\sigma_v^2}{2\pi G}.$$

This matter model has been traditionally used to describe gravitational lensing in systems such as individual galaxies and X-ray halos [20]. In addition, this mass distribution produces flat rotation curves in spiral galaxies, a classic marker for dark matter [18].

We are primarily interested in the viability of this model to describe the excess gravitational lensing usually associated to dark matter. Actually doing that involves reconstructing the mass distribution from a statistical analysis of the deformation and sheer of the 2D projected image of a galaxy cluster on the sky, which would take us quite far afield of our theoretical focus. For a classic introduction to that approach, see [19]. It is also true that

although the isothermal sphere is often a starting point for the analysis of such astrophysical systems, other models are commonly in use that appear to more accurately describe systems with large amounts of dark matter. Here, we will simply demonstrate that the mass distribution in this model is qualitatively similar to the distributions often found when performing more detailed analysis.

To determine the luminous matter in such clusters, X-ray detection of the hot intra-cluster medium is often used as a proxy. These  $\beta$ -models are parameterized by

$$\rho(r) = \rho_0 \left( 1 + \left( \frac{r}{r_c} \right) \right)^{-3\beta/2},$$

where  $\beta \approx 0.65$ , but varies for specific cases [43]. Figure 2 shows the minimum and maximum values of  $\beta$  in a particular recent survey [44]. Dark matter halos in such systems are often described with a Navarro-Frenk-White (MFW) profile, of the form

$$\rho(r) = \rho_0 \left\{ \frac{r}{r_c} \left( 1 + \frac{r}{r_c} \right)^{-2} \right\}.$$

We include these comparisons not as a strong argument that we expect it to have similar predictions in terms of lensing as either the  $\beta$ - or NFW-models, but only as a rough comparison. The fact that our analysis produced one of the most successful models for understanding matter distribution in extragalactic systems should be a strong argument for the validity of the essential approach. We also point out that this validity argument holds perfectly well for gravitational solitons in the weak field limit [25], since that also results in the singular isothermal sphere as a matter distribution.

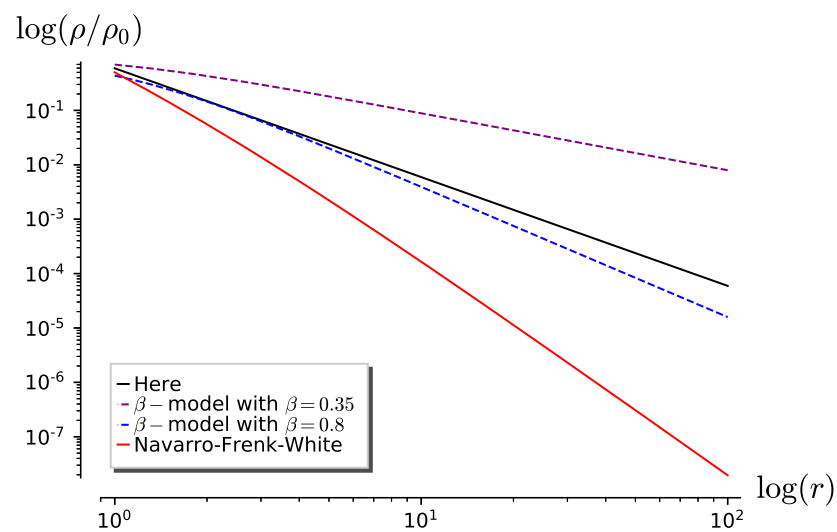


**Figure 2.** A qualitative comparison between the model in use here (the isothermal sphere) and two alternative models often used to describe the distribution of matter in galactic systems.

### 7. Summary

In this paper we have explored several examples of metrics on end-periodic manifolds, which are key constructions for the presentation of exotic smooth structure. By necessity, this approach feels “backwards” relative to the most common approach to the construction of spacetime models, because the information available about them is quite a bit different. Rather than particular symmetry conditions, or explicit equations of state, all we have to work with is the result of Taubes [29], that metrics on end-periodic manifolds can be constructed by a periodic transformation on building blocks (the Z-transformation). Once a building block is chosen, the matter model is inferred from the resulting metric, and reality conditions checked.

We have illustrated several examples using this approach, which includes the first potentially viable as a physical model. In the case of Exotic Kruskal, the resulting field equations were restrictively complex, although that case served to illustrate that the Z-transformation method (at least in the manner in which we are working with it) produces metrics with embedded conformal surfaces. Using this as a starting point, we generated a simpler building block which resulted in such a metric, and which we used to solve the field equations. The result was a well-known model, the singular isothermal sphere, but with a non-zero stress tensor. We also identified several places where our approach and results made contact with another recent study [25].

Of course, that matter distribution has been used in astrophysics for years, and is known to fail to describe most observational examples of dark matter. However, the association of what is essentially a monopole metric with a non-vacuum solution to the field equations represents a new connection, forged by considering the underlying spacetime to be an exotic smooth structure, presented as a end-periodic manifold. Perhaps more to the point, it is a slight variation on the original conjecture of Carl Brans—here the exotic smooth structure is not mimicking or generating matter, but rather an exotic smooth structure is shown to contain a standard matter distribution, previously known to the astronomical community. It is our hope that the initial work done here can be developed further to explore the parameter space of exotic smooth structures more completely, perhaps finding models which could stand on their own as explanations for dark matter that do not require the addition of exotic interactions or particles, but only exotic mathematics.

**Funding:** This research received no external funding.

**Institutional Review Board Statement:** Not applicable.

**Informed Consent Statement:** Not applicable.

**Acknowledgments:** The author would like to acknowledge several discussions with J. Overduin that informed several sections of this paper. In addition, there were many helpful comments and corrections provided by several of the reviewers and editors that greatly improved both the readability and applicability of this study. Finally, S. Barton assisted in checking and confirming several critical calculations.

**Conflicts of Interest:** The author declares no conflict of interest.

## Abbreviations

The following abbreviations are used in this manuscript:

CMB	Cosmic Microwave Background
FLRW	Freeman-Robertson-Lemaître-Walker
GR	General Relativity
LHC	Large Hadron Collider
MOND	Modified Newtonian Gravity
NFW	Navarro-Frenk-White

## Note

<sup>1</sup> The language “Z-transformation” comes from discrete signal processing, but seems an appropriate shorthand in this context.

## References

- Scorpan, A. *The Wild World of 4-Manifolds*; American Mathematical Society: Providence, RI, USA, 2005; p. xx+609.
- Asselmeyer-Maluga, T.; Brans, C.H. *Exotic Smoothness and Physics*; World Scientific Publishing Co. Pte. Ltd.: Hackensack, NJ, USA, 2007; p. xiv+322.
- Wald, R.M. *General Relativity*; University of Chicago Press: Chicago, IL, USA, 1984; p. xiii+491.
- Milnor, J. On manifolds homeomorphic to the 7-sphere. *Ann. Math.* **1956**, *64*, 399–405. [[CrossRef](#)]
- Freedman, M.H. The topology of four-dimensional manifolds. *J. Differ. Geom.* **1982**, *17*, 357–453. [[CrossRef](#)]
- Donaldson, S.K. An application of gauge theory to four-dimensional topology. *J. Differ. Geom.* **1983**, *18*, 279–315. [[CrossRef](#)]
- Witten, E. Monopoles and four-manifolds. *Math. Res. Lett.* **1994**, *1*, 769–796. [[CrossRef](#)]

8. Schleich, K.; Witt, D. Exotic spaces in quantum gravity. I. Euclidean quantum gravity in seven dimensions. *Class. Quantum Gravity* **1999**, *16*, 2447–2469. [[CrossRef](#)]
9. Salvetti, M. On the number of nonequivalent differentiable structures on 4-manifolds. *Manuscripta Math.* **1989**, *63*, 157–171. [[CrossRef](#)]
10. Duston, C.L. Exotic smoothness in four dimensions and Euclidean quantum gravity. *Int. J. Geom. Methods Mod. Phys.* **2011**, *8*, 459–484. [[CrossRef](#)]
11. Asselmeyer, T. Generation of source terms in general relativity by differential structures. *Class. Quantum Gravity* **1997**, *14*, 749–758. [[CrossRef](#)]
12. Asselmeyer-Maluga, T. Exotic smoothness and quantum gravity. *Class. Quantum Gravity* **2010**, *27*, 165002. [[CrossRef](#)]
13. Asselmeyer-Maluga, T.; Rosé, H. On the geometrization of matter by exotic smoothness. *Gen. Relativ. Gravit.* **2012**, *44*, 2825–2856. [[CrossRef](#)]
14. Asselmeyer-Maluga, T.; Brans, C.H. How to include fermions into general relativity by exotic smoothness. *Gen. Relativ. Gravit.* **2015**, *47*, 30. [[CrossRef](#)]
15. Brans, C.H. Localized exotic smoothness. *Class. Quantum Gravity* **1994**, *11*, 1785–1792. [[CrossRef](#)]
16. Freese, K. Review of Observational Evidence for Dark Matter in the Universe and in upcoming searches for Dark Stars. *EAS Publ. Ser.* **2009**, *36*, 113–126. [[CrossRef](#)]
17. Aaboud, M.; Aad, G.; Abbott, B.; Abbott, D.C.; Abdinov, O.; Abhayasinghe, D.K.; Abidi, S.H.; AbouZeid, O.S.; Abraham, N.L.; Abramowicz, H.; et al. Constraints on mediator-based dark matter and scalar dark energy models using  $\sqrt{s} = 13$  TeV pp collision data collected by the ATLAS detector. *J. High Energy Phys.* **2019**, *2019*, 142. [[CrossRef](#)]
18. Rubin, V.C.; Thonnard, N.; Ford, W.K., Jr. Rotational properties of 21 SC galaxies with a large range of luminosities and radii, from NGC 4605 / $R = 4$  kpc/ to UGC 2885 / $R = 122$  kpc/. *Astrophys. J.* **1980**, *238*, 471. [[CrossRef](#)]
19. Wambsganss, J. Gravitational Lensing in Astronomy. *Living Rev. Relativ.* **1998**, *1*, 12. [[CrossRef](#)]
20. Keeton, C.R. A Catalog of Mass Models for Gravitational Lensing. *arXiv* **2001**, arXiv:astro-ph/0102341.
21. Planck Collaboration; Aghanim, N.; Akrami, Y.; Arroja, F.; Ashdown, M.; Aumont, J.; Baccigalupi, C.; Ballardini, M.; Banday, A.J.; Barreiro, R.B.; et al. Planck 2018 results. I. Overview and the cosmological legacy of Planck. *Astron. Astrophys.* **2020**, *641*, A1. [[CrossRef](#)]
22. Asselmeyer-Maluga, T.; Brans, C.H. Cosmological anomalies and exotic smoothness structures. *Gen. Relativ. Gravit.* **2002**, *34*, 1767–1771. [[CrossRef](#)]
23. Asselmeyer-Maluga, T.; Król, J. How to obtain a cosmological constant from small exotic  $R^4$ . *Phys. Dark Universe* **2018**, *19*, 66–77. [[CrossRef](#)]
24. Asselmeyer-Maluga, T.; Brans, C. Smoothly Exotic Black Holes. In *Black Holes: Evolution, Theory and Thermodynamics*; Space Science, Exploration and Policies, Physics Research and Technology; NOVA Science Publisher: Hauppauge, NY, USA, 2012.
25. Asselmeyer-Maluga, T.; Król, J. Dark Matter as Gravitational Solitons in the Weak Field Limit. *Universe* **2020**, *6*, 234. [[CrossRef](#)]
26. Milgrom, M. Road to MOND: A novel perspective. *Phys. Rev. D* **2015**, *92*, 044014. [[CrossRef](#)]
27. Bekenstein, J.D. Relativistic gravitation theory for the modified Newtonian dynamics paradigm. *Phys. Rev. D* **2004**, *70*, 083509. [[CrossRef](#)]
28. Capozziello, S.; Laurentis, M.D.; Faraoni, V. A Bird’s Eye View of  $f(R)$ -Gravity. *Open Astron. J.* **2010**, *3*, 49–72. [[CrossRef](#)]
29. Taubes, C.H. Gauge theory on asymptotically periodic 4-manifolds. *J. Differ. Geom.* **1987**, *25*, 363–430. [[CrossRef](#)]
30. Asselmeyer-Maluga, T. Smooth Quantum Gravity: Exotic Smoothness and Quantum Gravity. In *At the Frontier of Spacetime; Fundamental Theories of Physics*; Springer International Publishing: Cham, Switzerland, 2016.
31. Visser, M. How to Wick rotate generic curved spacetime. *arXiv* **2017**, arXiv:1702.05572.
32. Carlip, S. Dimension and dimensional reduction in quantum gravity. *Class. Quantum Gravity* **2017**, *34*, 193001. [[CrossRef](#)]
33. Myrzakul, A.; Myrzakulov, R. On the Hojman conservation quantities in FRW Cosmology. *arXiv* **2016**, arXiv:1603.01611.
34. Duston, C.L. Using cosmic strings to relate local geometry to spatial topology. *Int. J. Mod. Phys. D* **2017**, *26*, 1750033–583. [[CrossRef](#)]
35. Hooft, G.T. Local conformal symmetry in black holes, standard model, and quantum gravity. *Int. J. Mod. Phys. D* **2017**, *26*, 1730006. [[CrossRef](#)]
36. Barriola, M.; Vilenkin, A. Gravitational field of a global monopole. *Phys. Rev. Lett.* **1989**, *63*, 341–343. [[CrossRef](#)] [[PubMed](#)]
37. The Sage Developers. SageMath, the Sage Mathematics Software System (Version 9.2). 2021. Available online: <https://www.sagemath.org> (accessed on 1 December 2021).
38. Maeda, H.; Martínez, C. Energy conditions in arbitrary dimensions. *Prog. Theor. Exp. Phys.* **2020**, *2020*, 043E02. Available online: <https://academic.oup.com/ptep/article-pdf/2020/4/043E02/33141458/ptaa009.pdf> (accessed on 1 December 2021). [[CrossRef](#)]
39. Pawar, D.; Patil, V.; Bayaskar, S. Spherically Symmetric Fluid Cosmological Model with Anisotropic Stress Tensor in General Relativity. *Int. Sch. Res. Not.* **2012**, *2012*, 10. [[CrossRef](#)]
40. Boonserm, P.; Ngampitipan, T.; Visser, M. Mimicking static anisotropic fluid spheres in general relativity. *Int. J. Mod. Phys. D* **2016**, *25*, 1650019. [[CrossRef](#)]
41. Ureña-López, L.A. Brief Review on Scalar Field Dark Matter Models. *Front. Astron. Space Sci.* **2019**, *6*. [[CrossRef](#)]
42. Binney, J.; Tremaine, S. *Galactic Dynamics*, 2nd ed.; Princeton Series in Astrophysics; Princeton University Press: Princeton, NJ, USA, 2008.

- 
43. Sarazin, C.L. X-ray emission from clusters of galaxies. *Rev. Mod. Phys.* **1986**, *58*, 1–115. [[CrossRef](#)]
  44. Croston, J.H.; Pratt, G.W.; Böhringer, H.; Arnaud, M.; Pointecouteau, E.; Ponman, T.J.; Saderson, A.J.R.; Temple, R.F.; Bower, R.G.; Donahue, M. Galaxy-cluster gas-density distributions of the representative XMM-Newton cluster structure survey (REXCESS). *Astron. Astrophys.* **2008**, *487*, 431–443. [[CrossRef](#)]